

Provided for non-commercial research and education use.
Not for reproduction, distribution or commercial use.



This article appeared in a journal published by Elsevier. The attached copy is furnished to the author for internal non-commercial research and education use, including for instruction at the authors institution and sharing with colleagues.

Other uses, including reproduction and distribution, or selling or licensing copies, or posting to personal, institutional or third party websites are prohibited.

In most cases authors are permitted to post their version of the article (e.g. in Word or Tex form) to their personal website or institutional repository. Authors requiring further information regarding Elsevier's archiving and manuscript policies are encouraged to visit:

<http://www.elsevier.com/copyright>



Contents lists available at ScienceDirect

Journal of Solid State Chemistry

journal homepage: www.elsevier.com/locate/jssc

Precipitation of $ALn(\text{CO}_3)_2 \cdot x\text{H}_2\text{O}$ and $\text{Dy}_2(\text{CO}_3)_3 \cdot x\text{H}_2\text{O}$ compounds from aqueous solutions for $A^+ = \text{Li}^+, \text{Na}^+, \text{K}^+, \text{Cs}^+, \text{NH}_4^+$ and $\text{Ln}^{3+} = \text{La}^{3+}, \text{Nd}^{3+}, \text{Eu}^{3+}, \text{Dy}^{3+}$

Violaine Philippini^{a,*}, Thomas Vercouter^a, Annie Chaussé^b, Pierre Vitorge^{a,b}

^a CEA Saclay DEN/DPC/SECR Laboratoire de Spéciation des Radionucléides et des Molécules, 91191 Gif-sur-Yvette, France

^b Laboratoire Analyse et Modélisation pour la Biologie et l'Environnement UMR 8587, Université d'Evry Val d'Essonne—CNRS, Boulevard F. Mitterrand, 91025 Evry cedex, France

ARTICLE INFO

Article history:

Received 13 September 2007

Received in revised form

22 April 2008

Accepted 27 April 2008

Available online 4 May 2008

Keywords:

Alkali metals

Ammonium

Lanthanides

Carbonate

XRD

Thermogravimetry

Precipitation

ABSTRACT

Double carbonates of lanthanide (*Ln*) and alkaline or ammonium (*A*) ions, noted $ALn(\text{CO}_3)_2 \cdot x\text{H}_2\text{O}$, were precipitated from concentrated A_2CO_3 aqueous solutions at room temperature and atmospheric pressure. Twelve hydrated compounds out of the twenty targeted ones have been obtained: $\text{Li}(\text{Nd or Eu})(\text{CO}_3)_2$, $\text{NaLa}(\text{CO}_3)_2$, $\text{KNd}(\text{CO}_3)_2 \cdot x\text{H}_2\text{O}$, $\text{Cs}(\text{La or Nd})(\text{CO}_3)_2$, $\text{NH}_4(\text{Nd, Eu or Dy})(\text{CO}_3)_2$, $\text{Dy}_2(\text{CO}_3)_3$ from concentrated A_2CO_3 solutions and $\text{Na}(\text{Nd, Eu or Dy})(\text{CO}_3)_2$ from concentrated AHCO_3 solutions. Although the trivalent lanthanide ions are often considered as analogs in solution, differences in their precipitation behaviour was observed, which is believed to have a kinetic origin in relation to the small differences in their ionic radii. The solid compounds were characterised by elemental analyses, thermogravimetry (TG), X-ray diffraction (XRD) and scanning electron microscope-energy dispersive spectroscopy (SEM-EDS). The powder diffraction patterns of nine solids were fitted using the tetragonal $P4/mmm$ *Laüe* class: $\text{LiNd}(\text{CO}_3)_2 \cdot x\text{H}_2\text{O}$: $a = (12.16 \pm 0.02) \text{ \AA}$, $c = (9.21 \pm 0.02) \text{ \AA}$, $\text{LiEu}(\text{CO}_3)_2 \cdot 3\text{H}_2\text{O}$: $a = (12.201 \pm 0.007) \text{ \AA}$, $c = (9.23 \pm 0.01) \text{ \AA}$, $\text{KNd}(\text{CO}_3)_2 \cdot x\text{H}_2\text{O}$: $a = (13.28 \pm 0.04) \text{ \AA}$, $c = (10.00 \pm 0.04) \text{ \AA}$, $\text{CsLa}(\text{CO}_3)_2 \cdot x\text{H}_2\text{O}$: $a = (10.82 \pm 0.02) \text{ \AA}$, $c = (8.18 \pm 0.02) \text{ \AA}$, $\text{CsNd}(\text{CO}_3)_2 \cdot x\text{H}_2\text{O}$: $a = (10.81 \pm 0.07) \text{ \AA}$, $c = (8.16 \pm 0.07) \text{ \AA}$ for $\text{NaLn}(\text{CO}_3)_2 \cdot x\text{H}_2\text{O}$: $a = (11.10 + 1.75r_{\text{Ln}^{3+}}) \text{ \AA}$ and $c = (8.60 + 1.13r_{\text{Ln}^{3+}}) \text{ \AA}$, where $r_{\text{Ln}^{3+}}$ is the ionic radius of Ln^{3+} for a coordination number of 8 ($r_{\text{La}^{3+}} = 1.16 \text{ \AA}$, $r_{\text{Nd}^{3+}} = 1.12 \text{ \AA}$, $r_{\text{Eu}^{3+}} = 1.07 \text{ \AA}$ and $r_{\text{Dy}^{3+}} = 1.03 \text{ \AA}$). It is proposed that all the $\text{NaLn}(\text{CO}_3)_2 \cdot x\text{H}_2\text{O}$ compounds are of very similar structure, as evidenced by their XRD patterns and by the linear variations of the lattice parameters with $r_{\text{Ln}^{3+}}$. The small differences in the lattice parameters can induce large modification of the precipitation pathways. Conversely, structural changes were evidenced within the A^+ series for $\text{ANd}(\text{CO}_3)_2 \cdot x\text{H}_2\text{O}$. $\text{Dy}_2(\text{CO}_3)_3 \cdot x\text{H}_2\text{O}$ was also obtained as a by-product. Its lattice parameters are in good agreement with $\text{Eu}_2(\text{CO}_3)_3 \cdot 3\text{H}_2\text{O}$ ones.

© 2008 Elsevier Inc. All rights reserved.

1. Introduction

The f-block elements usually have similar chemical behaviours when in the same oxidation state. Such analogies are typically used to estimate unknown stability constants for their aqueous complexes and solid compounds, assuming they have the same stoichiometries [1,2]. However, this type of analogy is still discussed for the aqueous carbonate complexes of lanthanides (*Ln*) or actinides (*An*) in the +3 oxidation state in concentrated solutions. Two stoichiometries have been proposed for their aqueous limiting carbonate complexes (the aqueous complex with the maximum carbonate per metal ratio): $\text{M}(\text{CO}_3)_3^{3-}$ and $\text{M}(\text{CO}_3)_4^{5-}$

[3]. In a recent capillary electrophoresis study we interpreted the variation of the electrophoretic mobilities across the *Ln* series as a change in the stoichiometries of the carbonate limiting complexes [4]. However, this technique does not give the stoichiometry of each complex. Interestingly, such stoichiometries have been determined by solubility measurements of $\text{NaM}(\text{CO}_3)_2 \cdot x\text{H}_2\text{O}$ compounds in concentrated carbonate aqueous solutions at room temperature and atmospheric pressure [5–9]. Unfortunately, the solubilities of $\text{AM}(\text{CO}_3)_2 \cdot x\text{H}_2\text{O}$ compounds, that actually control the room temperature solubility of lanthanides in concentrated carbonate aqueous solutions, have not been studied for a wide range of alkali metal cations (A^+) and M^{3+} cations, whereas it is tempting to use a similar methodology to determine the stoichiometry of the limiting complexes for a large set of Ln^{3+} cations. Indeed, well characterised solid compounds can be used in solubility measurements as probes of the stoichiometries and relative stabilities of aqueous species. In the present paper the

* Corresponding author. Fax: +33 1 69 08 54 11.

E-mail addresses: violaine.philippini@cea.fr, violaine.philippini@aliceadsl.fr (V. Philippini), pierre.vitorge@cea.fr (P. Vitorge).

synthesis procedures and the characterisations of such solids are reported. Note that since the solids need to be equilibrated with the aqueous solutions during the solubility measurements the solids must be prepared by precipitation from similar aqueous solutions than those used for the solubility measurements.

$ALn(CO_3)_2 \cdot xH_2O$ compounds are thermodynamically stable when equilibrated at room temperature with concentrated A_2CO_3 aqueous solutions. At lower A^+ or CO_3^{2-} concentrations, $Ln_2(CO_3)_3 \cdot xH_2O$ and $LnOHCO_3 \cdot xH_2O$ compounds can be the thermodynamically stable phases for high and low CO_2 partial pressures (pCO_2), respectively. pCO_2 and the $[Na^+]/\sqrt{CO_3^{2-}}$ ratios are the relevant experimental parameters to determine the stoichiometry of the thermodynamically stable solid compounds [10]. The preparation conditions and the corresponding results are often presented and discussed in terms of reactant ratios in the literature [11–20], while the relative stabilities of the solid compounds are governed by the A^+ , CO_3^{2-} and OH^- free aqueous concentrations. Indeed, the same solid compound was not obtained using similar reactant ratios but different $[Ln^{3+}]$ initial concentrations [11,21,22]. Moreover, $Ln_2(CO_3)_3 \cdot xH_2O$ and $LnOHCO_3 \cdot xH_2O$ might precipitate in concentrated Na_2CO_3 solutions, and slowly transforms into $NaLn(CO_3)_2 \cdot xH_2O$ within a few months at room temperature similarly to Am [6,7]. Thus, predominance diagrams are not sufficient to choose the precipitation conditions when kinetics allows the precipitation of a metastable compound. Unfortunately, it is not clear whether the kinetic behaviour of Am can be extrapolated to all An^{3+} and Ln^{3+} or not. Published experimental studies on $ALn(CO_3)_2 \cdot xH_2O$ compounds can give a few pieces of such kinetic information.

Various lanthanide (hydroxy)carbonates were precipitated from aqueous alkaline carbonate solutions [11–18,21–30]. Various stoichiometries were reported for the precipitated hydrated solid compounds: hydroxycarbonates ($Ln(OH)_y(CO_3)_z$), normal carbonates ($Ln_2(CO_3)_2$), double carbonates ($ALn(CO_3)_2$) and $A_3Ln(CO_3)_3$. Those various stoichiometries were proposed from the results of Ln chemical analysis of the precipitates and their mother liquors, but the precipitates were rarely characterised by X-ray diffraction (XRD). Sometimes, thermogravimetric (TG) analyses were performed, but not reported with enough experimental details to check the results and allow reinterpretation.

It remains unclear whether the same precipitation procedure can be used for the whole Ln series. The precipitation of Er^{3+} and Yb^{3+} from concentrated Na_2CO_3 solutions gave amorphous compounds at room temperature, whereas the same preparation method gave mixtures of $Ln_2O(CO_3)_2 \cdot xH_2O$ and $NaLn(CO_3)_2 \cdot xH_2O$ compounds for La and Ce [31]. Fannin [32] precipitated $KNd(CO_3)_2 \cdot xH_2O$ but failed to precipitate $KEu(CO_3)_2 \cdot xH_2O$ using the same procedure. Conversely, Faucherre et al. [33] obtained hydrated sodium and potassium double carbonates for all the lanthanides (except radioactive Pm which was not studied) by using the same precipitation conditions. The compositions of their solids were determined by A^+ , Ln^{3+} , CO_2 and H_2O analyses, but no XRD analysis was carried out.

For the synthesis of $ALn(CO_3)_2 \cdot xH_2O$ [8,9,11–19,21–24,31–40] contradictory results can partly be attributed to preparatory difficulties, namely hydrolysis of Ln^{3+} in basic carbonate solutions, oxidation of Ce^{3+} into Ce^{4+} or a poor control of the aqueous preparation conditions. Three different methods were employed: (i) precipitation of the compounds in A_2CO_3 or $AHCO_3$ solutions containing the metal salt [5,8,9,11–16,19,22,24,25,31–35,40], (ii) bubbling CO_2 in an aqueous suspension of Ln hydroxide ($Ln(OH)_3$) [19,37] and (iii) autoclaving mixtures of urea and Ln salts [19]. These methods gave similar results [19]. However, the nature of the precipitant (CO_3^{2-} or HCO_3^-), the temperature, the pressure, Ln^{3+} and CO_3^{2-} or HCO_3^- concentrations and the ageing period

influence the crystallisation, while the nature of the Ln salt does not seem to have any importance [41]. Note that the crystal chemistry of Ln carbonates is very limited, because the crystals suitable for structure determination are difficult to synthesise [42].

$ALn(CO_3)_2 \cdot xH_2O$ synthesis and characterisation are well documented for $A = Na$ [9,31–33,35,37]. Syntheses were also reported for $A = K$ [32,33,36,43,44] while to our best knowledge, hydrated $LiLn(CO_3)_2 \cdot xH_2O$ and $CsLn(CO_3)_2 \cdot xH_2O$ compounds have never been characterised. Poorly characterised compounds were reported for $NH_4Ln(CO_3)_2 \cdot xH_2O$. The literature clearly indicates that it is possible to precipitate some $ALn(CO_3)_2 \cdot xH_2O$ compounds from concentrated A_2CO_3 aqueous solutions at room temperature; but it is less clear whether all of them can be obtained by this method.

The Ln crystal ionic radii smoothly vary along the series ($r_{La^{3+}} = 1.16 \text{ \AA}$ to $r_{Lu^{3+}} = 0.97 \text{ \AA}$ for a coordination number of 8 [45]), due to the increase of the nuclear charge [46]. This radius contraction can lead to small variations of some properties: for example the diminution of the hydration number [47] and the modification of lattice parameters [34–36,44]. This contraction has also been proposed to explain the higher stabilities of $Ln_2(CO_3)_3$ for the heaviest lanthanides compared to the lightest ones [1]. In the present study, we try to precipitate a set of $ALn(CO_3)_2 \cdot xH_2O$ compounds from concentrated A_2CO_3 aqueous solutions at room temperature in order to carry out the solubility measurements presented elsewhere [3,48]. Thus, well crystallised compounds are not especially expected. We have chosen four representative lanthanides with quite different ionic radii La, Nd, Eu and Dy and five counter-ions Li^+ , Na^+ , K^+ , Cs^+ and NH_4^+ . Firstly, further details on published syntheses and the procedures used to synthesise and characterise the solid compounds are presented (Section 2). The solid characterisations (elemental analyses, thermal analyses, XRD and SEM analyses are then described (Section 3). Finally the results of the syntheses and the characterisations among the Ln and A series are discussed, since we succeeded in precipitating $NaLn(CO_3)_2 \cdot xH_2O$ compounds for the four chosen Ln , and $ANd(CO_3)_2 \cdot xH_2O$ compounds for the five counter-ions. Analogies and differences within the Ln series are also discussed (Section 4).

2. Solid precipitation procedures

2.1. Published procedures

- $LiLn(CO_3)_2 \cdot xH_2O$ compounds were precipitated by mixing Li_2CO_3 and either $LnCl_3$ or $Ln(NO_3)_3$ for Ce, Pr, Nd, Sm and Eu. For the other lanthanides, this method led to $Ln_2(CO_3)_3 \cdot xH_2O$ and amorphous compounds for lanthanides heavier than Eu [34]. Autoclaving a stoichiometric mixture of Li_2CO_3 and $Ln_2(C_2O_4)_3 \cdot xH_2O$ gave the non-hydrated $LiLn(CO_3)_2$ compounds for all the lanthanides. The dehydrated compounds were characterised by elemental analyses, XRD and Fourier transform infrared spectroscopy. Monoclinic lattices were proposed for all the lanthanides but with various Z (number of molecules per unit cell): $Z = 4$ for La to Gd and $Z = 8$ for Tb to Lu.
- $NaLn(CO_3)_2$ synthesis is well documented [9,31–33,35,37]. The hydrated compounds are often obtained by precipitation, and some XRD patterns are reported for hydrated double carbonates of Nd, Sm, Eu, Gd and Dy [9,31,32,37]. Dehydrated $NaLn(CO_3)_2$ were obtained by heating the hydrated compounds in autoclaves [35]. The dehydrated compounds are crystalline and their structures were accurately determined whereas the hydrated polycrystalline compounds were not characterised.

The hydrated compounds are supposed to crystallise in a tetragonal lattice [31,37] whereas the non-hydrated ones crystallised in orthorhombic (La to Gd) or monoclinic (Tb to Lu) lattices [35]. The structure break was observed for Gd for non-hydrated compounds [35], no difference was observed for the hydrated compounds.

- Potassium double carbonate syntheses were reported in five studies, hydrated [32,33,43] or not [36,44]. Two different lattices were reported for polycrystalline non-hydrated compounds, an orthorhombic one for La to Nd, and a monoclinic one for Sm to Lu [36]. Those compounds have been obtained from $KLn(CO_3)_2 \cdot xH_2O$ dehydrated in autoclave, they were not characterised before dehydration. Non-hydrated single crystals were also obtained for Nd, Gd, Dy, Ho and Yb in an autoclave [44]. Seven JCPDS files are referenced for the non-hydrated compounds and one for $KGd(CO_3)_2 \cdot 3H_2O$ (00-031-1015), starting from the polycrystalline powder prepared by Faucher et al. [33] single crystals of $KGd(CO_3)_2 \cdot 3H_2O$ were precipitated after several months of equilibration in the mother liquor [43]. The diffraction pattern of the latter is very different from the $NaLn(CO_3)_2 \cdot xH_2O$ ones (00-030-1223, 00-030-1240, 00-031-1288, 00-031-1291, 00-054-0641 and 00-053-1065) and from the diffraction pattern of $KNd(CO_3)_2 \cdot xH_2O$ obtained by Fannin [32] which looks like that of $NaLn(CO_3)_2 \cdot xH_2O$.
- $CsPr(CO_3)_2$ was synthesised by thermolysing $Cs_2(H_3O)Pr(CH_3COO)_6$ in an autoclave [49]. No precipitation of such compounds in aqueous solutions was reported.
- $NH_4Ln(CO_3)_2 \cdot xH_2O$ compounds were proposed for $Ln = La, Ce, Pr, Nd, Eu, Gd, Tb, Dy, Er, Ho, Tm$ and Lu , but without XRD characterisation [11–15,18,25,27,28] or XRD characterisation showing amorphous solids [12].

2.2. Materials

All the experiments were performed at room temperature ($23 \pm 1^\circ C$). Millipore deionised water (Alpha-Q, 18.2 M Ω cm) was used throughout the experiments. The carbonate or hydrogencarbonate solutions were prepared from weighted amounts of Li_2CO_3 (Sigma, Sigmaultra $\geq 99\%$), Na_2CO_3 (VWR, Normapur $\geq 99.9\%$), $NaHCO_3$ (VWR, Normapur $\geq 99.5\%$), K_2CO_3 (VWR, Normapur $\geq 99.9\%$), $KHCO_3$ (Aldrich $\geq 99.99\%$), Cs_2CO_3 (Aldrich $\geq 99.95\%$), $CsHCO_3$ (Aldrich $\geq 99.9\%$) or NH_4HCO_3/NH_2COONH_4 (VWR, Normapur) used without further purification. The resulting aqueous solutions were titrated with 1 mol L^{-1} HCl (Merck, Titrisol) or with 1 mol L^{-1} NaOH (VWR-prolabo, Normadose)

aqueous solutions. The Ln solutions were prepared from weighted amounts of $La(NO_3)_3 \cdot 6H_2O$ (VWR, Rectapur $\geq 99.99\%$), $Nd(NO_3)_3 \cdot 6H_2O$ (Johnson Matthey $\geq 99.9\%$), $Eu(NO_3)_3 \cdot 5H_2O$ (Aldrich $\geq 99.99\%$) and $Dy(NO_3)_3 \cdot 5H_2O$ (Johnson Matthey $\geq 99.9\%$).

2.3. $ALn(CO_3)_2 \cdot xH_2O$ syntheses

Three different methods were used to precipitate the twelve obtained solid compounds since we did not succeed to use a single method for all the lanthanides. This was quite expected from the literature (as outlined in the Introduction). All the mixtures were kept in polytetrafluoroethylene (PTFE) flasks and were continuously shaken (reciprocating motion). Experimental conditions of the syntheses are summarised in Table 1.

2.3.1. The A_2CO_3 and $AHCO_3$ methods

We systematically tried to prepare $ALn(CO_3)_2 \cdot xH_2O$ compounds by mixing 8 mL of A_2CO_3 or $AHCO_3$ solutions ($0.5\text{--}2 \text{ mol L}^{-1}$) with $0.32\text{--}1 \text{ mL}$ of $Ln(NO_3)_3$ solutions ($0.7\text{--}3.6 \text{ mol L}^{-1}$). Finally, nine hydrated solid phases were obtained namely $NaLn(CO_3)_2 \cdot xH_2O$ ($Ln = La, Nd, Eu$ and Dy), $CsLn(CO_3)_2 \cdot xH_2O$ ($Ln = La$ and Nd) and $NH_4Ln(CO_3)_2 \cdot xH_2O$ ($Ln = Nd, Eu$ and Dy). The sodium double carbonates were kept at least for 82 days in their mother liquor before being analysed. The ammonium and caesium double carbonates were kept for 118 days in their mother liquor.

2.3.2. The frozen saturated Li_2CO_3 method

Since the precipitation of lithium double carbonates failed with the general procedure, we used von Kalz et al. [34] method: $LiNd(CO_3)_2 \cdot xH_2O$ and $LiEu(CO_3)_2 \cdot 3H_2O$ were obtained by a slow (2 h) dropwise addition of 8–10 mL of a frozen saturated Li_2CO_3 solution to a frozen 0.1 mol L^{-1} $Ln(NO_3)_3$ solution. Each of the two solutions were cooled in an ice bath during the whole procedure. The final solution was magnetically stirred during 12 h in the ice bath. A cooled solution of Li_2CO_3 was used since the solubility of this salt increases when the temperature decreases. The resulting lithium double carbonates were kept at least for 82 days in their mother liquor before being analysed.

2.3.3. The N_2 bubbling method

Since the precipitation of potassium double carbonates failed with the general procedure, we tried to precipitate $KLn(CO_3)_2 \cdot xH_2O$ compounds following Fannin's procedure [32], 195 mL of 0.1 mol L^{-1} K_2CO_3 solution were mixed with 5 mL of 0.2 mol L^{-1} $Ln(NO_3)_3$ aqueous solution as for the " A_2CO_3 method". The mother

Table 1
Experimental conditions of the $ALn(CO_3)_2 \cdot xH_2O$ syntheses

	$[A_2CO_3]$ $[AHCO_3]$, mol L^{-1}	$V_{A_2CO_3}$ V_{AHCO_3} , mL	$[Ln^{3+}]$, mol L^{-1}	$V_{Ln^{3+}}$, mL	Method
$LiNd(CO_3)_2 \cdot xH_2O$	Saturated	10	0.100	1.250	Frozen
$LiEu(CO_3)_2 \cdot 3H_2O$	Saturated	8	0.105	1.500	Frozen
$NaLa(CO_3)_2 \cdot xH_2O$	1.000	8	0.696	1.000	A_2CO_3
$NaNd(CO_3)_2 \cdot 5H_2O$	0.500	8	2.245	0.320	$AHCO_3$
$NaEu(CO_3)_2 \cdot 5H_2O$	0.500	8	2.385	0.320	$AHCO_3$
$NaDy(CO_3)_2 \cdot 6H_2O$	0.500	8	2.266	0.320	$AHCO_3$
$KNd(CO_3)_2 \cdot xH_2O$	0.100	195	0.200	5.000	N_2 bubbling
$CsLa(CO_3)_2 \cdot xH_2O$	2.000	8	3.582	0.320	A_2CO_3
$CsNd(CO_3)_2 \cdot xH_2O$	2.000	8	3.564	0.320	A_2CO_3
$NH_4Nd(CO_3)_2 \cdot H_2O$	0.613 ^a	8	0.867	0.320	A_2CO_3
$NH_4Eu(CO_3)_2 \cdot H_2O$	0.613 ^a	8	0.847	0.320	A_2CO_3
$NH_4Dy(CO_3)_2$	0.613 ^a	8	0.851	0.320	A_2CO_3

^a The commercial product is obtained as a white fibrous mass, which consists of a mixture of ammonium hydrogen carbonate (NH_4HCO_3) and ammonium carbamate (NH_2COONH_4) in equimolar proportions. The value given for the carbonate concentration corresponds to the concentration of the mixture (the solution was prepared in a 100 mL volumetric flask which contained 9.623 g of NH_4HCO_3/NH_2COONH_4).

liquor was then subjected to nitrogen bubbling during 2 h. The flask was hermetically closed and it was kept in a nitrogen glove-box. The solid initially aggregated in cloudy masses for the four lanthanides. Acicular crystals crystallised 7 weeks later only for Nd, the resulting $\text{KNd}(\text{CO}_3)_2 \cdot x\text{H}_2\text{O}$ compound was then analysed.

2.3.4. $\text{Dy}_2(\text{CO}_3)_3$ synthesis

As a by-product of our attempt to prepare $\text{NaDy}(\text{CO}_3)_2 \cdot x\text{H}_2\text{O}$ using the “ Na_2CO_3 method”, we obtained $\text{Dy}_2(\text{CO}_3)_3$, which is certainly not the thermodynamically stable product in these conditions. This was not especially unexpected for kinetic reason as reported in the Introduction. Since its powder pattern had never been published, but appeared to be very similar to that of $\text{Eu}_2(\text{CO}_3)_3 \cdot 3\text{H}_2\text{O}$, its lattice parameters were determined in Section 3.3. This compound was precipitated by adding 1 mL of 2.2 mol L^{-1} $\text{Dy}(\text{NO}_3)_3 \cdot 5\text{H}_2\text{O}$ solution to 24 mL of 0.1 mol L^{-1} NaHCO_3 solution.

2.4. Solid characterisation

The solid compounds were filtered after an equilibration period of a few days, and just before being analysed, in order to avoid any evolution since double carbonates are renowned unstable in dried and/or hot atmospheres [8,19,31,40]. Filtration was performed with a nitrocellulose Whatman $0.2 \mu\text{m}$ membrane. The collected solid was rinsed with deionised water. Since ageing period from a few days [31,35,36] to a few months [33] were observed for the crystallisation of the double carbonates, the age of the sample is given for each analysis.

2.4.1. Elemental analyses

The Ln and A concentrations were measured by inductively coupled plasma optical emission spectroscopy (ICP-OES Perkin Elmer Optima 2000 DV spectrometer), except for the $\text{NH}_4\text{Ln}(\text{CO}_3)_2 \cdot x\text{H}_2\text{O}$ compounds. A weighted amount of $\text{ALn}(\text{CO}_3)_2 \cdot x\text{H}_2\text{O}$ was dissolved in an appropriate volume of 0.5 mol L^{-1} HNO_3 solution to neutralise CO_3^{2-} and to keep strong acidity. The detector was calibrated using standard solutions (Spex, Certiprep, 2% HNO_3) diluted in 0.5 mol L^{-1} nitric acid. The measurements were carried out using two emission wavelengths for each Ln and one for the alkali metal. Six replicates were performed for each element at each wavelength. The standard deviations on the Ln or A concentration determinations were in the 0.5–4% range. The analyses were made just after the XRD phase identification, the age of the solid compounds was the same as for the XRD analysis.

2.4.2. Thermal analyses

Thermal analysis was used to measure H_2O , NH_3 and CO_2 contents in the solid compounds. TG and differential thermal analysis (DTA) were performed using a SETARAM TAG 24 TG apparatus. An amount of 11–25 mg of $\text{ALn}(\text{CO}_3)_2 \cdot x\text{H}_2\text{O}$ compounds was placed into an alumina crucible. The crucible was maintained at 35°C during 90 min under argon prior to being tared. It was heated from 35°C to 1200°C at a rate of 6°C min^{-1} . This temperature of 1200°C remained constant for 20 min. Finally, the samples were cooled down to 40°C at $10^\circ\text{C min}^{-1}$. The whole procedure was carried out in a pure Ar atmosphere to reduce buoyancy.

In most of the published studies, TG–DTA was used to determine the water content of the solid compounds [13–15,23,31,33], but not their carbonate content, which decomposition occurs at higher temperatures. For this reason, the samples were heated to 1200°C .

Mass spectral analysis of the gases emitted during the thermal decomposition (i.e. H_2O , CO_2 , NH_3 , N_2 , O_2 , Ar) was carried out using an Omnistar GSD 300 O (Pfeiffer). Firstly, the atomic masses were scanned in the 1–200 atomic mass unit (a.m.u.) range in order to qualitatively detect the main emitted gases and to make sure that no unexpected species were eliminated. The results of these first acquisitions were used to choose the a.m.u. range of interest. The gas analysis was not quantitative since a part of the gas emitted in the furnace did not enter the capillary that linked the thermobalance to the gas mass spectrometer. We did not obtain usable results for $\text{CsLn}(\text{CO}_3)_2 \cdot x\text{H}_2\text{O}$ compounds because the decomposition of volatile Cs_2CO_3 occurred at about 610°C , and altered the thermocouples. Moreover, the m/z range covered by the mass spectrometer was not large enough to analyse the Cs containing gas. $\text{ALn}(\text{CO}_3)_2 \cdot x\text{H}_2\text{O}$ compounds have been kept between 215 and 232 days in their mother liquor before being analysed by TG, except $\text{NaLa}(\text{CO}_3)_2 \cdot x\text{H}_2\text{O}$ (45 days) and $\text{LiEu}(\text{CO}_3)_2 \cdot 3\text{H}_2\text{O}$ (82 days).

2.4.3. Microscopic analyses

The purity and the morphology of the solid samples were checked with a JEOL JSM-6100 SEM. The residua of some TG–DTA analyses were also analysed by EDS to determine their qualitative elemental composition. This analysis was made just after the XRD phase identification, the age of the solid compounds was the same as for the XRD analysis.

2.4.4. XRD analyses

Preparing the samples by sieving the powders with a $80\text{-}\mu\text{m}$ sieve led to a shift of the peaks because of the thickness of the samples. Thus, the sample preparation procedure was modified: a small fraction of washed wet samples was laid down on a non-diffracting silicon sample holder, and analysed right after it dried. This may cause a preferential orientation and the loss of some peaks if the grains are not spherical. To avoid texture effects, the samples were spinning all along the experiments. SEM-EDS analyses did not evidence any particular grain shape, that could cause the loss of some peaks. The diffraction data were collected on a X'Pert pro Panalytical X-ray diffractometer with $\text{CoK}\alpha_1$ radiation (1.78901 \AA), produced at 45 kV and 40 mA. The spinning samples were scanned over a 2θ range of $6\text{--}65^\circ$ by steps of 0.02° , with a time step of 1.2 s. The solid phases were identified using the X'Pert HighScore software supported by the Powder Diffraction File 2-database. The double carbonates were analysed after an equilibration time of 49 days ($\text{KNd}(\text{CO}_3)_2 \cdot x\text{H}_2\text{O}$), 82 days ($\text{NaLn}(\text{CO}_3)_2 \cdot x\text{H}_2\text{O}$ and $\text{LiLn}(\text{CO}_3)_2 \cdot x\text{H}_2\text{O}$) or 118 days ($\text{CsLn}(\text{CO}_3)_2 \cdot x\text{H}_2\text{O}$ and $\text{NH}_4\text{Ln}(\text{CO}_3)_2 \cdot x\text{H}_2\text{O}$).

The powder diffraction patterns were fitted using the less constrained tetragonal $P4/mmm$ *Laüe* class by a least-squares analysis of the d -spacings between our experimental data and Mochizuki's ones, who proposed a tetragonal unit cell for $\text{NaLn}(\text{CO}_3)_2 \cdot x\text{H}_2\text{O}$ ($\text{Ln} = \text{Nd}, \text{Sm}, \text{Gd}, \text{Dy}$) [31]. The h, k, l indices for the extra peaks were attributed thanks to the U-FIT software [50] using the lattice parameters previously determined.

3. Results

3.1. Syntheses

We succeeded to precipitate twelve $\text{ALn}(\text{CO}_3)_2 \cdot x\text{H}_2\text{O}$ compounds from concentrated aqueous carbonate or hydrogen carbonate solutions for four lanthanides ($\text{Ln} = \text{La}, \text{Nd}, \text{Eu}$ and Dy), and four alkali metals ($A = \text{Li}, \text{Na}, \text{K}, \text{Cs}$) and NH_4 . Among various by-products, the non-referenced $\text{Dy}_2(\text{CO}_3)_3 \cdot x\text{H}_2\text{O}$ normal carbonate

was also obtained. One hundred and four syntheses were carried out, thirty-nine gave $ALn(\text{CO}_3)_2 \cdot x\text{H}_2\text{O}$. The products were analysed by XRD after different equilibration periods (2–422 days) to control their evolutions. Solid transformations were only detected for $\text{LiNd}(\text{CO}_3)_2 \cdot x\text{H}_2\text{O}$ and $\text{KNd}(\text{CO}_3)_2 \cdot x\text{H}_2\text{O}$.

We attempted to precipitate all the chosen $ALn(\text{CO}_3)_2 \cdot x\text{H}_2\text{O}$ compounds from carbonate aqueous solutions, since it corresponds to the thermochemical conditions where the solubility is controlled by $ALn(\text{CO}_3)_2 \cdot x\text{H}_2\text{O}$ compounds at room temperature and atmospheric pressure, as outlined in the Introduction. The “ A_2CO_3 and AHCO_3 ” methods were systematically tested, varying the reactant concentrations: $[\text{A}_2\text{CO}_3]$ ranged from 0.08 to 1.95 mol L^{-1} , $[\text{AHCO}_3]$ ranged from 0.48 to 2 mol L^{-1} and $[\text{Ln}(\text{NO}_3)_3]$ ranged from 0.005 to 0.14 mol L^{-1} in the mother liquor. Nine hydrated double carbonates were obtained by these methods (Table 1). Three compounds ($\text{NaNd}(\text{CO}_3)_2 \cdot 5\text{H}_2\text{O}$, $\text{NaEu}(\text{CO}_3)_2 \cdot 5\text{H}_2\text{O}$ and $\text{NaDy}(\text{CO}_3)_2 \cdot 6\text{H}_2\text{O}$) were precipitated from hydrogen carbonate solutions. The XRD patterns of some precipitates also showed the formation of amorphous compounds, normal carbonates, hydroxycarbonates or mixtures identified by comparison with referenced patterns. (i) It appeared that $\text{La}_2(\text{CO}_3)_3$ was easily prepared in hydrogen carbonate solutions whatever the alkali metal ion. In 0.1 mol L^{-1} NaHCO_3 and 0.09 mol L^{-1} $\text{Ln}(\text{NO}_3)_3$ solutions, $\text{Ln}_2(\text{CO}_3)_3 \cdot x\text{H}_2\text{O}$ precipitated for the four chosen lanthanides, but a mixture of $\text{La}_2(\text{CO}_3)_3$ and $\text{NaLa}(\text{CO}_3)_2 \cdot x\text{H}_2\text{O}$ was obtained. (ii) $\text{Dy}_2(\text{CO}_3)_3 \cdot x\text{H}_2\text{O}$ was obtained for the first time. This compound was identified thanks to its experimental powder diffraction pattern, which appeared to be similar to the reference pattern of $\text{Eu}_2(\text{CO}_3)_3 \cdot 3\text{H}_2\text{O}$. (iii) NdOHCO_3 was also obtained by precipitation from Li_2CO_3 or K_2CO_3 solutions (0.015 mol L^{-1} $\text{Nd}(\text{NO}_3)_3 \cdot 6\text{H}_2\text{O}/0.6 \text{ mol L}^{-1}$ Li_2CO_3 or 0.03 mol L^{-1} $\text{Nd}(\text{NO}_3)_3 \cdot 6\text{H}_2\text{O}/0.08 \text{ mol L}^{-1}$ K_2CO_3 or 0.05 mol L^{-1} $\text{Nd}(\text{NO}_3)_3 \cdot 6\text{H}_2\text{O}/0.1 \text{ mol L}^{-1}$ K_2CO_3 solutions).

We did not succeed to reproduce some published syntheses, mainly in potassium and ammonium media. Using the “ A_2CO_3 and AHCO_3 methods” Kalz et al. [36] and Faucherre et al. [33] obtained $\text{KLn}(\text{CO}_3)_2$ for La, Ce, Pr and Nd, and for the whole series of lanthanides, respectively. Since no information was given on the concentrations and the volumes of the various solutions, twenty-four tests were achieved varying the concentration of metal salt (0.01 – 0.13 mol L^{-1}) and the concentration of carbonate (0.005 – 2 mol L^{-1}) in the mother liquor. Only amorphous solid compounds were obtained, except for Nd: $\text{NdOH}(\text{CO}_3)$ precipitated from a 0.44 mol L^{-1} $\text{K}_2\text{CO}_3/0.05 \text{ mol L}^{-1}$ $\text{Nd}(\text{NO}_3)_3 \cdot 6\text{H}_2\text{O}$ solution after two months. Mzareulishvili et al. [13,18] managed to precipitate $\text{KLa}(\text{CO}_3)_2 \cdot 4\text{H}_2\text{O}$, $\text{CsLa}(\text{CO}_3)_2 \cdot 2\text{H}_2\text{O}$ and $\text{KDy}(\text{CO}_3)_2 \cdot 3\text{H}_2\text{O}$ from 0.025 mol L^{-1} Ln solutions and A_2CO_3 , the $n = [\text{CO}_3^{2-}]_{\text{ini}}/[\text{Ln}^{3+}]_{\text{ini}}$ ratios were 20, 10 and 3, respectively. Only amorphous compounds were obtained reproducing these procedures. However, none of these authors carried out XRD analysis on the hydrated compounds, the nature of the compounds have been proposed thanks to elemental analyses or XRD on dehydrated compounds [36]. Using the same experimental conditions as for $\text{CsLa}(\text{CO}_3)_2 \cdot x\text{H}_2\text{O}$ and $\text{CsNd}(\text{CO}_3)_2 \cdot x\text{H}_2\text{O}$ compounds (i.e. similar Ln and A concentrations) no precipitate was obtained for Eu nor for Dy. In ammonium carbonate solutions, an unidentified crystalline compound was obtained for La (seven peaks (d (Å), intensity (%)) = (8.27, 4), (11.86, 100), (23.86, 8), (36.16, 7), (39.73, 1), (45.56, 1) and (51.74, 1)).

We obtained lithium and potassium double carbonates by slightly modifying the “ A_2CO_3 method”: the “frozen saturated Li_2CO_3 method” and the “ N_2 bubbling method” were used. $\text{LiNd}(\text{CO}_3)_2 \cdot x\text{H}_2\text{O}$, $\text{LiEu}(\text{CO}_3)_2 \cdot 3\text{H}_2\text{O}$ and $\text{KNd}(\text{CO}_3)_2 \cdot x\text{H}_2\text{O}$ were obtained. However, $\text{LiNd}(\text{CO}_3)_2 \cdot x\text{H}_2\text{O}$ appeared to be unstable: a few days after its XRD analysis, i.e. after atmospheric CO_2 entered into the flask, it transformed into NdOHCO_3 in its mother liquor (characterised by XRD). Similarly, $\text{KNd}(\text{CO}_3)_2 \cdot x\text{H}_2\text{O}$ transformed

into an amorphous phase. Using the same experimental method as for $\text{LiNd}(\text{CO}_3)_2 \cdot x\text{H}_2\text{O}$ and $\text{LiEu}(\text{CO}_3)_2 \cdot 3\text{H}_2\text{O}$, a gel was obtained for La and Dy, and amorphous phases precipitated from the potassium aqueous solutions for La, Eu and Dy using the same experimental method as for $\text{KNd}(\text{CO}_3)_2 \cdot x\text{H}_2\text{O}$.

3.2. The solid stoichiometries

The weight loss curve of $\text{NaEu}(\text{CO}_3)_2 \cdot 5\text{H}_2\text{O}$ and the curves that represent the emission of H_2O and CO_2 during the solid decomposition are shown in Fig. 1. This TG result is first described. Only a selected part of the TG analysis is presented since no weight loss was observed during the cooling part (after 18000 s). For clarity, the DTA signal is not superimposed on the graphs since each weight loss can be described by an endothermic reaction. After the initial plateau, a second plateau starts at about 245°C . The corresponding mass loss (23.2%) can be interpreted by dehydration which occurs in two stages: 2 molecules per Eu were emitted at 120°C and 3.1 molecules between 120 and 245°C . The water loss is followed by the loss of one CO_2 from 245 to 475°C . The emission of the second CO_2 occurs in three stages: ($\frac{1}{4}$, $\frac{1}{4}$ and $\frac{1}{2}$, respectively) from 475 to 1150°C . On the DTA curves, sharp endothermic peaks are associated with the water loss and the first emission of CO_2 (g). The last steps are only determined by TG and gas analyses, because of the too low signal-to-noise ratio of the DTA signal. The melting of Na_2CO_3 causes an endothermic effect at about 860°C with no modification of the TG signal.

The preliminary gas analysis did not evidence the emission of other gases than those expected: the atmosphere gases (N_2 and O_2) are emitted during the furnace purge, then H_2O and CO_2 are emitted during the solid decomposition, and Ar is emitted during the whole analysis since it was carried out in a pure Ar atmosphere to reduce buoyancy. Two m/z are charted, 18 and 44 which correspond to H_2O^+ and CO_2^+ , respectively. The TG curve can be divided into six different parts corresponding to five peaks on the gas spectrometric assays (the water emission is represented by a unique peak which splits). The weight loss and the nature of the emitted gas are consistent with the following reaction scheme:

- (1) $\text{NaEu}(\text{CO}_3)_2 \cdot 5\text{H}_2\text{O} \rightarrow \text{NaEu}(\text{CO}_3)_2 \cdot 3\text{H}_2\text{O} + 2\text{H}_2\text{O}(\text{g})$
- (2) $\text{NaEu}(\text{CO}_3)_2 \cdot 3\text{H}_2\text{O} \rightarrow \text{NaEu}(\text{CO}_3)_2 + 3\text{H}_2\text{O}(\text{g})$
- (3) $\text{NaEu}(\text{CO}_3)_2 \rightarrow \frac{1}{2}\text{Na}_2\text{CO}_3 + \frac{1}{2}\text{Eu}_2\text{O}_2\text{CO}_3 + \text{CO}_2(\text{g})$

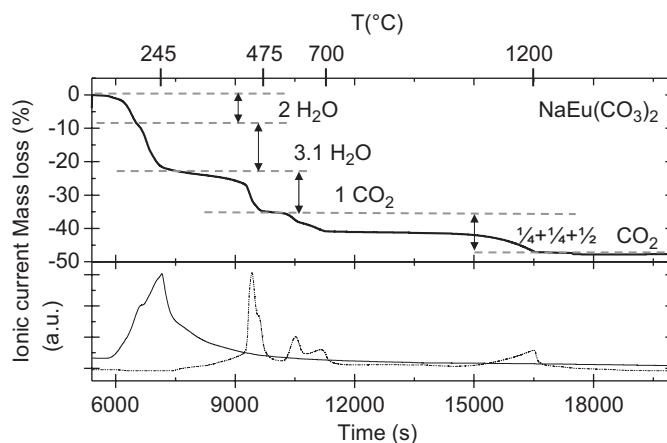
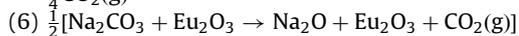
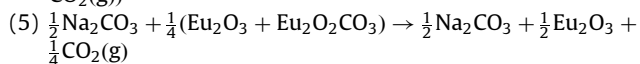
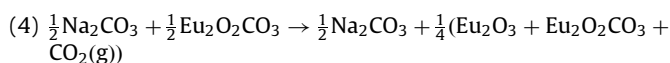
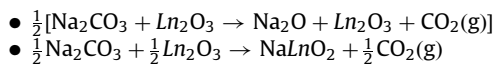


Fig. 1. Thermogravimetric and corresponding mass spectrometry analysis of $\text{NaEu}(\text{CO}_3)_2 \cdot 5\text{H}_2\text{O}$. The weight loss is represented in the upper part of the graph and the emissions of water (solid line) and carbon dioxide (dashed line) are represented in the bottom part.



The stoichiometric coefficients of carbonate and water in the precipitate were determined from the weight loss and the nature of the emitted gas. A ± 0.2 uncertainty is evaluated on the stoichiometric coefficients resulting from the graphical determination of the plateaux on the TG signal.

The water loss occurs in two steps, which suggests the presence of both free and bound water. The bound water is eliminated at higher temperature. These results confirm those of Mochizuki and Faucherre [31,33]. The intermediate steps (3–5) have been clearly identified by Schweer et al. [35] but they obtained a $1 : \frac{1}{2} : \frac{1}{2}$ ratio for the CO_2 loss whereas we obtained a $1 : \frac{1}{4} : \frac{1}{4} : \frac{1}{2}$ one. For the last step, two reactions have been proposed:

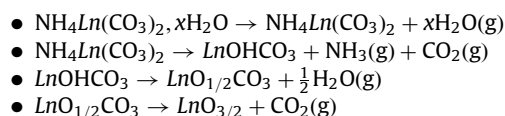


The reaction forming the NaLnO_2 intermediate was regarded as the most probable [38]. We analysed the residuum of $\text{NaEu}(\text{CO}_3)_2 \cdot 5\text{H}_2\text{O}$ by XRD and SEM. Eu_2O_3 was clearly evidenced by XRD (Fig. 2), which suggests that the last step is step 6. Although Na_2O was not observed by XRD, the SEM analysis revealed the presence of sodium in the residuum. Na_2O is indeed an amorphous solid, and it represents less than 5% in mass of the residuum, which is lower than the threshold of the XRD apparatus.

The TG curves and the gas analyses for $\text{NaLn}(\text{CO}_3)_2 \cdot x\text{H}_2\text{O}$ ($\text{Ln} = \text{Nd}$ and Dy) are similar to those of $\text{NaEu}(\text{CO}_3)_2 \cdot 5\text{H}_2\text{O}$ whereas the analysis of $\text{NaLa}(\text{CO}_3)_2 \cdot x\text{H}_2\text{O}$ is slightly different (Fig. 3). For the latter, the total weight loss is superior to that of the other compounds, and CO_2 emissions started at the beginning of the experiment simultaneously to H_2O release. It may be attributed to the transformation of a portion of $\text{NaLa}(\text{CO}_3)_2 \cdot x\text{H}_2\text{O}$ into $\text{La}_2(\text{CO}_3)_3$ as reported by Fannin et al. [40] on drying $\text{NaNd}(\text{CO}_3)_2 \cdot 6\text{H}_2\text{O}$ and $\text{NaEu}(\text{CO}_3)_2 \cdot 6\text{H}_2\text{O}$. They reported that those two double carbonates evolved within six days. The alteration time might be smaller for $\text{NaLa}(\text{CO}_3)_2 \cdot x\text{H}_2\text{O}$ since all the compounds were air-dried during a night and only this one altered. Moreover, the CO_2 removal of $\text{NaDy}(\text{CO}_3)_2 \cdot 6\text{H}_2\text{O}$ occurs with a $1 : \frac{1}{2} : \frac{1}{2}$ ratio whereas a $1 : \frac{1}{4} : \frac{1}{4} : \frac{1}{2}$ one was obtained with Eu and Nd, i.e. steps 4 and 5 are simultaneous. It can be noted that the lighter the Ln , the higher the temperature of decomposition. For this reason, a maximum temperature of 1400°C (instead of 1200°C) was needed to reach the final plateau for the analysis of $\text{NaLa}(\text{CO}_3)_2 \cdot x\text{H}_2\text{O}$. The XRD and SEM analyses of the residua of

$\text{NaNd}(\text{CO}_3)_2 \cdot 5\text{H}_2\text{O}$ and $\text{NaDy}(\text{CO}_3)_2 \cdot 6\text{H}_2\text{O}$ confirmed the last step of the decomposition. $\text{LiEu}(\text{CO}_3)_2 \cdot 3\text{H}_2\text{O}$ behaves the same way as the sodium compounds, but the water loss occurs in a single step, which can be explained by the absence of free water. The melting of Li_2CO_3 causes an endothermic effect at about 720°C . However, during the cooling phase, a sharp exothermic peak appears at 970°C without sample mass variation, which might be caused by a transformation of Li_2O , since it did not appear on the $\text{NaLn}(\text{CO}_3)_2 \cdot x\text{H}_2\text{O}$ TG curves.

The behaviour of the ammonium carbonates appears to be more complex. NH_3 emission is evidenced by a peak at $m/z = 15$ (NH_3^+) on the mass spectrometric gas analysis. This complex behaviour is usual since the decomposition of ammonium forms ammonia, and the remaining proton combines with oxygen to form water, as proposed in this possible reaction scheme:



These proposed reactions can be simultaneous. Due to the simultaneous emission of various gases, quantitative analysis of the experimental results on $\text{NH}_4\text{Ln}(\text{CO}_3)_2 \cdot x\text{H}_2\text{O}$ compounds was not possible. Measuring the total weight loss, the hydration number of the $\text{NH}_4\text{Ln}(\text{CO}_3)_2 \cdot x\text{H}_2\text{O}$ compounds was extrapolated, assuming that the carbonate stoichiometric coefficient in the solid compounds is $\nu_{\text{CO}_2} = 2$. Since the total weight losses are 43.3%, 46.4% and 44.4% for $\text{NH}_4\text{Nd}(\text{CO}_3)_2 \cdot \text{H}_2\text{O}$, $\text{NH}_4\text{Eu}(\text{CO}_3)_2 \cdot \text{H}_2\text{O}$ and $\text{NH}_4\text{Dy}(\text{CO}_3)_2$ respectively, their calculated hydration numbers are: 0.8 ± 0.2 , 1.3 ± 0.2 and 0.1 ± 0.2 , respectively.

The thermal decomposition of $\text{LiNd}(\text{CO}_3)_2 \cdot x\text{H}_2\text{O}$ and $\text{KNd}(\text{CO}_3)_2 \cdot x\text{H}_2\text{O}$ was not studied because they evolved after a few weeks in their mother liquor.

The temperatures of decomposition are summarised in Table 2, and the stoichiometric composition of the double carbonates are presented in Table 3. It can be noted that the number of free water molecules is not an integer.

The microscopic analysis of the solid compounds did not reveal any particular shape of the grains. The absence of impurity was checked (absence of other lanthanides or alkali metals in the solid compounds). The experimental SEM-EDS patterns or maps are not shown since they did not suggest any new interpretation.

The following stoichiometries are proposed for the twelve compounds prepared in this study: $\text{LiNd}(\text{CO}_3)_2 \cdot x\text{H}_2\text{O}$, $\text{LiEu}(\text{CO}_3)_2 \cdot 3\text{H}_2\text{O}$, $\text{NaLa}(\text{CO}_3)_2 \cdot x\text{H}_2\text{O}$, $\text{NaNd}(\text{CO}_3)_2 \cdot 5\text{H}_2\text{O}$, $\text{NaEu}(\text{CO}_3)_2 \cdot 5\text{H}_2\text{O}$, $\text{NaDy}(\text{CO}_3)_2 \cdot 6\text{H}_2\text{O}$, $\text{KNd}(\text{CO}_3)_2 \cdot x\text{H}_2\text{O}$, $\text{CsLa}(\text{CO}_3)_2 \cdot \text{H}_2\text{O}$, $\text{CsNd}(\text{CO}_3)_2 \cdot \text{H}_2\text{O}$, $\text{NH}_4\text{Nd}(\text{CO}_3)_2 \cdot \text{H}_2\text{O}$, $\text{NH}_4\text{Eu}(\text{CO}_3)_2 \cdot \text{H}_2\text{O}$ and $\text{NH}_4\text{Dy}(\text{CO}_3)_2$.

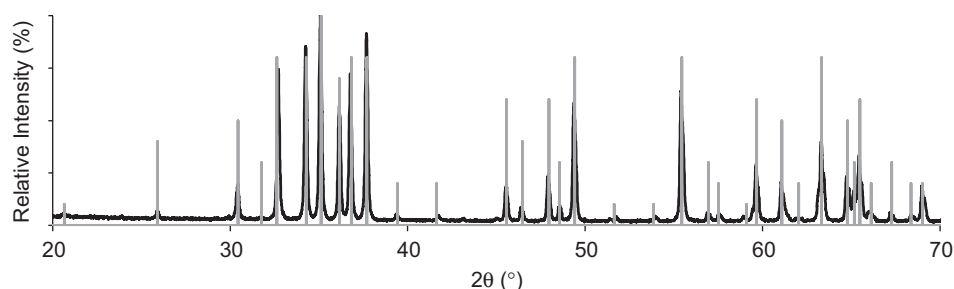


Fig. 2. XRD analysis of $\text{NaEu}(\text{CO}_3)_2 \cdot 5\text{H}_2\text{O}$ residuum after its thermal decomposition. The experimental pattern is in black, and JCPDS 00-012-0384 Eu_2O_3 reference file is in grey.

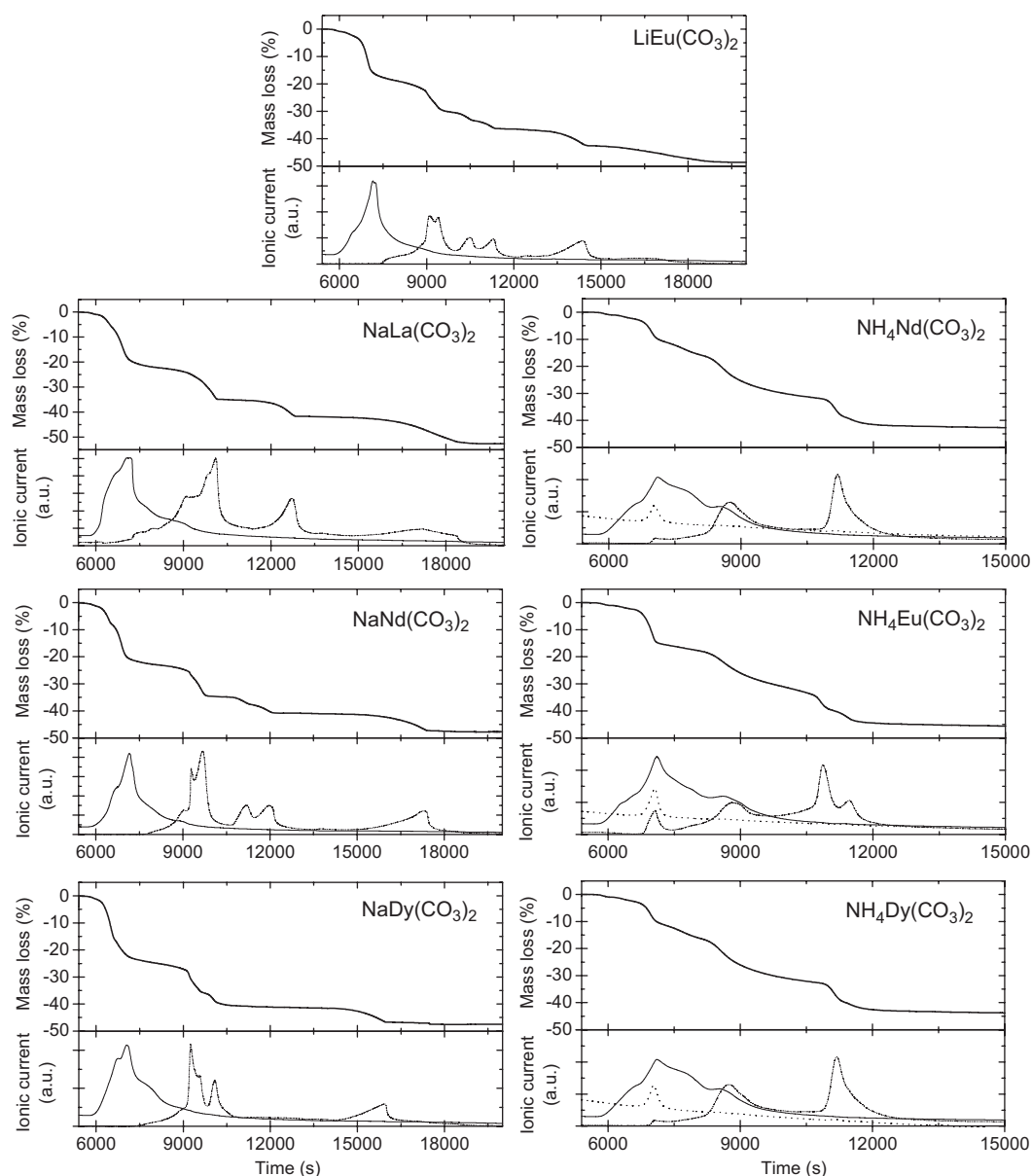


Fig. 3. Thermogravimetric analyses of lithium, sodium and ammonium double carbonates. The weight loss (upper figures) and the emissions of water (solid line), carbon dioxide (dashed line) and ammonia (dotted line) are represented.

Table 2

Temperatures of H₂O and CO₂ emissions during the TG analyses (in °C)

	Water loss		CO ₂ loss			
	Step 1	Step 2	Step 3	Step 4	Step 5	Step 6
NaN ₂ (CO ₃) ₂ ·5H ₂ O	< 120	120–265	265–475	475–615	615–700	700–1200
NaEu(CO ₃) ₂ ·5H ₂ O	< 120	120–245	245–475	475–550	550–615	615–1150
NaDy(CO ₃) ₂ ·6H ₂ O	< 130	130–265	265–425		425–580	580–1100
LiEu(CO ₃) ₂ ·3H ₂ O		215	215–430	430–545	545–630	630–950

3.3. Solid phase identification and lattice parameters

The experimental XRD patterns are quite similar, with only slight shifts of the lines (Fig. 4). The differences between the patterns can be attributed to the radius of the alkali metal or to the hydration number (assuming that whatever the alkali metal ion or the hydration number, solid compounds crystallise into the

same lattice). The solid phases have been identified by comparison to the JCPDS files, when existing. The *d*-spacings and the relative intensities of the diffraction peaks taken from the experimental published results are very different from one to the other. Twenty-nine JCPDS files of $ALn(CO_3)_2$ are referenced in the PDF2 database (JCPDS numbers: 00-030-1223, 00-030-1240, 00-031-1015, 00-031-1288, 00-031-1291, 00-035-0956 to

00-035-0961, 00-036-0547, 00-036-0548, 00-036-0730 to 00-036-0735, 00-053-1065, 00-054-0641, 07-072-2203, 01-084-2415, 01-086-2158, 01-088-1419 to 01-088-1423). They were extracted from nine publications [31,35–37,43,44,49,51,52]. Nineteen of these JCPDS files concern $\text{NaLn}(\text{CO}_3)_2$ compounds, among them, six described hydrated $\text{NaLn}(\text{CO}_3)_2 \cdot x\text{H}_2\text{O}$; but a doubtful or blank quality has been assigned to those files. These six referenced files are quite similar, but in the experimental pattern reported by Runde et al. [37] there are some extra peaks: an intense one (\approx

Table 3

Analyses of the solid stoichiometries: A and Ln concentrations are measured by ICP-OES and water and carbonate stoichiometric coefficients are determined by TG analyses

$A\text{Ln}(\text{CO}_3)_2 \cdot x\text{H}_2\text{O}$	$\frac{[\text{Ln}^{3+}]}{[\text{A}^+]}$	$\nu_{\text{CO}_3^{2-}}$	$\nu_{\text{H}_2\text{O}}$	$\nu_{\text{H}_2\text{O}}$ (bound water)
$\text{LiNd}(\text{CO}_3)_2 \cdot x\text{H}_2\text{O}$	No assay			
$\text{LiEu}(\text{CO}_3)_2 \cdot 3\text{H}_2\text{O}$	1.0 ± 0.1	2.0 ± 0.2	2.8 ± 0.2	2.8 ± 0.2
$\text{NaLa}(\text{CO}_3)_2 \cdot x\text{H}_2\text{O}$	0.97 ± 0.06			
$\text{NaNd}(\text{CO}_3)_2 \cdot 5\text{H}_2\text{O}$	1.03 ± 0.05	2.0 ± 0.2	4.8 ± 0.2	3.1 ± 0.2
$\text{NaEu}(\text{CO}_3)_2 \cdot 5\text{H}_2\text{O}$	1.02 ± 0.06	2.1 ± 0.2	5.1 ± 0.2	3.1 ± 0.2
$\text{NaDy}(\text{CO}_3)_2 \cdot 6\text{H}_2\text{O}$	1.06 ± 0.06	1.9 ± 0.2	5.8 ± 0.2	2.1 ± 0.2
$\text{KNd}(\text{CO}_3)_2 \cdot x\text{H}_2\text{O}$	No assay			
$\text{CsLa}(\text{CO}_3)_2 \cdot x\text{H}_2\text{O}$	0.9 ± 0.1			
$\text{CsNd}(\text{CO}_3)_2 \cdot x\text{H}_2\text{O}$	1.04 ± 0.05			
$\text{NH}_4\text{Nd}(\text{CO}_3)_2 \cdot \text{H}_2\text{O}$			0.8 ± 0.2	
$\text{NH}_4\text{Eu}(\text{CO}_3)_2 \cdot \text{H}_2\text{O}$			1.3 ± 0.2	
$\text{NH}_4\text{Dy}(\text{CO}_3)_2$			0.1 ± 0.2	

20%) and a lot of small ones ($\leq 3\%$). The Bragg reflections given in Table 1 of Ref. [37] do not match the experimental diffraction powder pattern presented in Fig. 1 of Ref. [37]. The 00-054-0641 reference file is based on the table thus the reference pattern is quite different from the experimental one. There are neither reference files, nor published diffraction patterns, for double carbonates with $A \neq \text{Na, K}$. We calculate the lattice parameters of the obtained solid compounds according to the $P4/mmm$ Laue class.

The experimental patterns of $\text{NaLn}(\text{CO}_3)_2 \cdot x\text{H}_2\text{O}$ present five narrow peaks, which compare with the reference files 00-030-1223, 00-030-1240, 00-031-1288 and 00-031-1291 and with published data [9,31,32]. Two representative references are superimposed on the experimental diffraction patterns to make the comparison easier (Fig. 4).

$\text{LiEu}(\text{CO}_3)_2 \cdot 3\text{H}_2\text{O}$ XRD experimental pattern compares with $\text{NaLn}(\text{CO}_3)_2 \cdot x\text{H}_2\text{O}$ ones with a slight shift of the five peaks. $\text{LiNd}(\text{CO}_3)_2 \cdot x\text{H}_2\text{O}$ diffraction pattern shows a lot of small broad peaks, it seems that this solid transforms into NdOHCO_3 on drying or water washing. It is much less crystalline than $\text{LiEu}(\text{CO}_3)_2 \cdot 3\text{H}_2\text{O}$. A part of $\text{KNd}(\text{CO}_3)_2 \cdot x\text{H}_2\text{O}$ experimental pattern compares with $\text{NaLn}(\text{CO}_3)_2 \cdot x\text{H}_2\text{O}$ ones, but there are some additional peaks that might evidence an additional phase (the peaks attributed to this secondary phase are marked with a * in Fig. 4). Since the double carbonate evolved before being analysed by ICP-OES, we cannot ascertain its composition. $\text{KNd}(\text{CO}_3)_2 \cdot x\text{H}_2\text{O}$ was here evidenced by its XRD diffraction pattern maybe in a mixture. All our extra peaks had been reported by Delaunay et al. [43] for

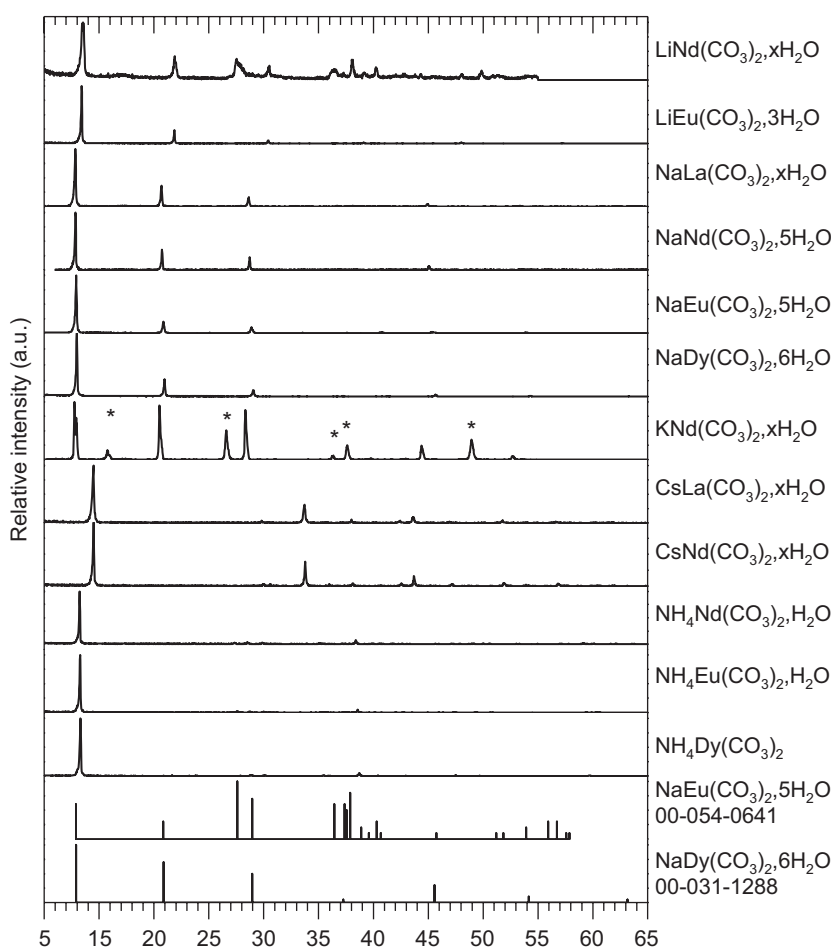


Fig. 4. Powder XRD patterns of hydrated $\text{ALn}(\text{CO}_3)_2 \cdot x\text{H}_2\text{O}$ solid compounds.

KGd(CO₃)₂·3H₂O. Unfortunately, they did not show their diffraction pattern and the intensities of the peaks were only qualitatively described (average, low, very low, very very low). The referenced diffraction pattern of KGd(CO₃)₂·3H₂O showed a dozen of other extra peaks, four of them were the most intense ones, they are not present on our powder pattern. The lattice parameters of KNd(CO₃)₂·xH₂O have been calculated with the non-starred peaks only. Some extra peaks appeared on the diffraction powder patterns of CsLn(CO₃)₂·xH₂O, whereas there is almost a single intense peak for NH₄Ln(CO₃)₂·xH₂O.

From the experimental powder patterns, the unit cell parameters of ALn(CO₃)₂·xH₂O compounds have been calculated, except for the ammonium salts because of the small number of peaks (Tables 4–6). If various indices correspond to the same peak, the less probable indices are put in brackets.

One can note that since the most probable indices are always (*h*, 0, 0), the indices put in brackets are used to determine the *c* parameter. Thus, *c* is less accurately determined than the *a* parameter. This methodology can cause a systematic error on the *c* determination, but since it was applied to all the studied solid compounds, it gives a consistent general trend. The influence of the Ln radii on the lattice parameters is moderate and consistent with the Ln contraction: the shift of the first peak, that can be indexed (*h*, *k*, *l*) = (1, 0, 0) ≈ *a* for a tetragonal cell, is small: *d*_{NaLa} = 13.111 Å, *d*_{NaNd} = 13.075 Å, *d*_{NaEu} = 12.981 Å, *d*_{NaDy} = 12.93 Å, or *d*_{CsLa} = 10.84 Å, *d*_{CsNd} = 10.81 Å (one can note that the solid formulae have been shortened). However, the influence on the alkali metal radius on the lattice parameters seems more important *d*_{LiNd} = 12.05 Å, *d*_{NaNd} = 13.075 Å, *d*_{KNd} = 13.24 Å, *d*_{NH₄Nd} = 12.502 Å and *d*_{CsNd} = 10.81 Å. The lattice parameter for LiNd(CO₃)₂·xH₂O and KNd(CO₃)₂·xH₂O compounds are much more uncertain since the powder quantity laid on the silicon holder was too important, as a consequence a shift of the peak can appear. For the lithium, sodium and potassium double carbonates the expected tendency is respected since the *a*-length of the cells increases with the ionic radius of the alkali metal ion (*r*_{Li⁺} = 0.68 Å, *r*_{Na⁺} = 0.97 Å and *r*_{K⁺} = 1.33 Å [45]). In ammonium and caesium media this tendency is no more observed (*r*_{NH₄⁺} = 1.45 Å and *r*_{Cs⁺} = 1.67 Å [45]), this may be due to a large change of the hydration number or a slight modification of the Bravais lattice.

The diffraction powder pattern of Dy₂(CO₃)₃·xH₂O (Fig. 5) had never been published; but it is very similar to the Eu₂(CO₃)₃·3H₂O referenced one, which was synthesised by using ammonium hydrogen carbonate as precipitant. We indexed the XRD data in the monoclinic system similarly to Liu et al. [53]. Dy₂(CO₃)₃·xH₂O

lattice parameters, determined with U-FIT computer program, are: *a* = 11.84 ± 0.03 Å, *b* = 9.19 ± 0.02 Å, *c* = 8.26 ± 0.04 Å and β = 107.3 ± 0.2°. They are a little bit shorter than those of

Table 5

Experimental powder X-ray diffraction *d* values, intensities and *hkl* indices for CsLn(CO₃)₂·xH₂O compounds

<i>hkl</i>	CsLa(CO ₃) ₂ ·xH ₂ O		CsNd(CO ₃) ₂ ·xH ₂ O	
	<i>d</i> (Å)	<i>I</i> (%)	<i>d</i> (Å)	<i>I</i> (%)
100	10.84	100	10.81	100
211	4.17	3	4.14	3
112, 300	3.61	33	3.60	36
311	3.15	3	3.14	4
222	2.79	2	2.78	3
400, 302	2.71	9	2.70	15
411	2.50	1	2.49	2
402	2.26	3	2.25	4
500, 430, 332	2.16	1	2.16	1
511	2.06	2	2.05	3
611	1.74	2	1.73	2
<i>a</i> (Å)	(10.82 ± 0.02)		(10.81 ± 0.07)	
<i>c</i> (Å)	(8.18 ± 0.02)		(8.16 ± 0.07)	
<i>V</i> (Å ³)	958		954	

Table 6

Experimental powder X-ray diffraction *d* values and intensities for NH₄Ln(CO₃)₂·xH₂O compounds

NH ₄ Nd(CO ₃) ₂ ·H ₂ O		NH ₄ Eu(CO ₃) ₂ ·H ₂ O		NH ₄ Dy(CO ₃) ₂	
<i>d</i> (Å)	<i>I</i> (%)	<i>d</i> (Å)	<i>I</i> (%)	<i>d</i> (Å)	<i>I</i> (%)
12.502	100.0	12.441	100.0	12.369	100.0
4.615	2.8	4.565	2.5	4.508	0.5
4.387	2.8	4.355	2.0	4.332	1.9
4.154	3.0	4.137	1.7	4.115	1.5
3.446	1.9	3.427	0.7	3.408	1.1
3.116	9.1	3.101	5.4	3.088	4.5
2.573	0.4	2.963	0.6	2.943	0.4
2.491	1.0	2.558	0.5	2.538	0.2
2.383	1.2	2.473	0.3	2.470	0.7
2.309	0.5	2.369	0.6	2.355	0.4
1.968	1.8	1.958	0.6	1.948	0.9
1.936	0.7	1.923	0.3	1.913	0.3
1.706	0.7	1.698	0.3	1.690	0.5

Table 4

Experimental powder X-ray diffraction (XRD) *d* values, intensities and *hkl* indices for lithium, sodium and potassium double carbonates. The powder diffraction patterns were fitted using the less constrained tetragonal *P4/mmm* Laue class

<i>hkl</i>	LiNd(CO ₃) ₂ ·xH ₂ O		LiEu(CO ₃) ₂ ·3H ₂ O		NaLa(CO ₃) ₂ ·xH ₂ O		NaNd(CO ₃) ₂ ·5H ₂ O		NaEu(CO ₃) ₂ ·5H ₂ O		NaDy(CO ₃) ₂ ·6H ₂ O		KNd(CO ₃) ₂ ·xH ₂ O	
	<i>d</i> (Å)	<i>I</i> (%)	<i>d</i> (Å)	<i>I</i> (%)										
100	12.05	100.0	12.193	100.0	13.111	100.0	13.075	100.0	12.981	100.0	12.93	100.0	13.24	100.0
200	6.10	39.5	6.103	20.8	6.560	36.0	6.542	30.6	6.489	19.9	6.45	31.4	6.64	93.0
300 (112)	4.06	17.7	4.067	6.2	4.373	13.8	4.357	13.4	4.327	9.1	4.30	11.1	4.43	86.0
400	3.05	8.7	3.050	1.6										
500 (430, 332)	2.44	6.9	2.440	2.1	2.623	3.8	2.614	4.1	2.596	1.9	2.58	2.6	2.66	24.5
600 (522, 224)	^a		2.034	0.7	2.184	1.2	2.178	1.0	2.163	0.4	2.15	0.7	2.21	6.1
<i>a</i> (Å)	(12.16 ± 0.02)		(12.201 ± 0.007)		(13.114 ± 0.003)		(13.070 ± 0.007)		(12.980 ± 0.001)		(12.89 ± 0.04)		(13.28 ± 0.04)	
<i>c</i> (Å)	(9.21 ± 0.02)		(9.23 ± 0.01)		(9.90 ± 0.03)		(9.90 ± 0.01)		(9.81 ± 0.01)		(9.76 ± 0.01)		(10.00 ± 0.04)	
<i>V</i> (Å ³)	1362		1374		1703		1691		1653		1621		1763	

^a LiNd(CO₃)₂·xH₂O XRD pattern was obtained just before it evolved. Unfortunately, too much powder was placed on the silicon disc which led to a slight shift of the peaks. Moreover, the diffraction pattern was collected between 2θ = 5° and 50°. For this reason no peak is reported for the last indices.

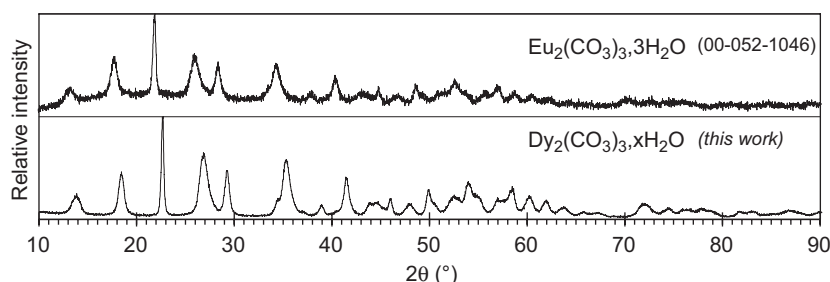


Fig. 5. Comparison of $\text{Dy}_2(\text{CO}_3)_3 \cdot x\text{H}_2\text{O}$ diffraction pattern with $\text{Eu}_2(\text{CO}_3)_3 \cdot 3\text{H}_2\text{O}$ referenced one.

Table 7

Experimental powder X-ray diffraction d values, intensities and hkl indices for $\text{Dy}_2(\text{CO}_3)_3 \cdot 3\text{H}_2\text{O}$

hkl	d (Å)	I (%)	hkl	d (Å)	I (%)
$10\bar{1}$	7.440	24	042	1.981	37
101	5.611	44	$31\bar{4}$	1.962	22
020	4.574	100	600	1.884	20
$\bar{3}01$	3.866	63	050	1.841	30
121	3.558	47	$\bar{6}22$	1.792	23
221	3.034	20	$\bar{2}51$	1.748	17
$32\bar{1}$	2.964	56	$\bar{5}33$	1.699	11
131	2.697	13	350	1.651	8
013	2.539	40	$54\bar{2}$	1.620	6
$33\bar{1}$	2.400	16	$15\bar{3}, 54\bar{3}$	1.526	14
$50\bar{1}$	2.369	17	$324, 64\bar{2}$	1.482	10
040	2.301	18	$55\bar{1}, 81\bar{1}$	1.450	10
041	2.207	15	550	1.426	10
141	2.131	27	$62\bar{5}, 632$	1.371	7
$50\bar{3}$	2.033	23	$225, 820$	1.351	7
			$51\bar{6}, 154$	1.305	9

h , k and l are overlined when they are negative.

$\text{Eu}_2(\text{CO}_3)_3 \cdot 3\text{H}_2\text{O}$ ($a = 11.983 \text{ \AA}$, $b = 9.300 \text{ \AA}$, $c = 8.2429 \text{ \AA}$ and $\beta = 107.643^\circ$) consistently with the Ln contraction (Table 7).

4. Discussion

The precipitation of double carbonates was achieved by different synthesis methods depending on the nature of the $Ln(\text{III})$ ion. This observation is consistent with the results of Mochizuki et al. [31] who failed to synthesise hydrated $\text{NaLn}(\text{CO}_3)_2 \cdot x\text{H}_2\text{O}$ for La, Er, Yb, while they succeeded for Nd, Sm, Gd and Dy by using a similar method. In the present work, sodium double carbonates, $\text{NaLn}(\text{CO}_3)_2 \cdot x\text{H}_2\text{O}$, were obtained for the four tested lanthanides (La, Nd, Eu and Dy), all with the same structure as evidenced by their XRD patterns (Fig. 4). Solubility batch experiments have been carried out with these solid phases, which has enabled a direct investigation of the aqueous carbonate complexes of the $Ln(\text{III})$ [3,48]. The $\text{NaLn}(\text{CO}_3)_2 \cdot x\text{H}_2\text{O}$ compounds of Nd, Eu, and Dy have been precipitated in concentrated hydrogen carbonate solutions, while precipitation in more dilute hydrogen carbonate solutions produced normal carbonates $\text{Ln}_2(\text{CO}_3)_3 \cdot x\text{H}_2\text{O}$. The formation conditions of these two types of solid compounds is consistent with their thermodynamic stabilities. Conversely, La behaves differently than Nd, Eu, and Dy, since $\text{La}_2(\text{CO}_3)_3 \cdot x\text{H}_2\text{O}$ precipitate easily in concentrated hydrogen carbonate solutions (Section 3.1) while it should be less stable than $\text{NaLa}(\text{CO}_3)_2 \cdot x\text{H}_2\text{O}$ in such conditions, by analogy with the other lanthanides. It is likely that $\text{La}_2(\text{CO}_3)_3 \cdot x\text{H}_2\text{O}$ is metastable in our

conditions. Such a behaviour was observed for $\text{Am}_2(\text{CO}_3)_3$ prepared in aqueous carbonate solutions: it was shown to transform into the more stable phase $\text{NaAm}(\text{CO}_3)_2 \cdot x\text{H}_2\text{O}$ within a few months or a few days at 50°C [6,7]. Even small differences in the chemistry of the Ln ions in hydrogen carbonate solutions, might induce different precipitation pathways, as demonstrated elsewhere [3]. As a consequence, at a short equilibration time, hydrogen carbonate solutions oversaturated with La may generate another precipitate than $\text{NaLa}(\text{CO}_3)_2 \cdot x\text{H}_2\text{O}$ (i.e. $\text{La}_2(\text{CO}_3)_3 \cdot x\text{H}_2\text{O}$), which would be kinetically favoured.

The synthesis of $\text{NaLn}(\text{CO}_3)_2 \cdot x\text{H}_2\text{O}$ compounds appeared to be easier than that of the lithium, potassium, caesium and ammonium double carbonates. The crystal ionic radii of the lanthanides ($r_{\text{La}^{3+}} = 1.16 \text{ \AA}$ to $r_{\text{Lu}^{3+}} = 0.97 \text{ \AA}$) are close to the crystal radius of sodium ($r_{\text{Na}^+} = 0.97 \text{ \AA}$), which might facilitate the crystallisation of $\text{NaLn}(\text{CO}_3)_2 \cdot x\text{H}_2\text{O}$ compounds.

It appeared that the length of the cell edges and their volumes vary linearly with the ionic radii of Ln^{3+} for $\text{NaLn}(\text{CO}_3)_2 \cdot x\text{H}_2\text{O}$ compounds (Fig. 6). Although the number of valence electrons increases among the Ln series, such correlations are expected for Ln^{3+} hard cations since binding is essentially driven by electrostatic interactions. A linear variation of the cell parameters with the ionic radius was reported by several authors [31,34–36]. Nevertheless, when two different structures were proposed for the same alkali metal with various lanthanides [34–36] the linear plot of the lattice parameters did not fit to the experimental results and two different slopes were proposed. Since a unique slope fit our experimental data, the four studied lanthanides crystallised into the same lattice, consistently with the hypothesis of a tetragonal $P4/mmm$ unique Laue class used to determine the lattice parameters. There are two published determinations of lattice parameters for similar structures. The lattice parameters obtained by Mochizuki et al. [31] for hydrated $\text{NaLn}(\text{CO}_3)_2 \cdot x\text{H}_2\text{O}$ with $Ln = \text{Nd}, \text{Sm}, \text{Gd}$ and Dy, and the lattice parameters obtained by Runde et al. [37] for $\text{NaM}(\text{CO}_3)_2 \cdot 5\text{H}_2\text{O}$ with $M = \text{Nd}, \text{Eu}, \text{Am}$ compare with our results (Fig. 6). Note that the Am data of Runde et al. for $\text{NaAm}(\text{CO}_3)_2 \cdot 5\text{H}_2\text{O}$ fall on the line of the $Ln(\text{III})$ data, which enable to estimate the An(III) lattice parameters.

The number of bound water is two in $\text{NaDy}(\text{CO}_3)_2 \cdot 2\text{H}_2\text{O}$, while it is three for the lighter (bigger) lanthanides (Table 3). Since no important changes in the XRD patterns were observed (Fig. 4), water molecules are probably not directly bound to Ln^{3+} , they are rather expected to be in interlayers, which size can vary with the size of Ln^{3+} .

We obtained $\text{ANd}(\text{CO}_3)_2 \cdot x\text{H}_2\text{O}$ compounds for $A^+ = \text{Li}^+, \text{Na}^+, \text{K}^+, \text{Cs}^+$ and NH_4^+ . In this series, it appeared that the values of the lattice parameters increased with the crystal ionic radii for Li^+, Na^+ and K^+ , whereas for Cs^+ and NH_4^+ the value of the a parameter is no more correlated to the ionic radii. This can be attributed to slight structural changes consistently with the XRD patterns (Fig. 4). Note that $\text{CsLa}(\text{CO}_3)_2 \cdot x\text{H}_2\text{O}$ and $\text{CsNd}(\text{CO}_3)_2 \cdot x\text{H}_2\text{O}$ compounds have very similar XRD patterns, while the XRD

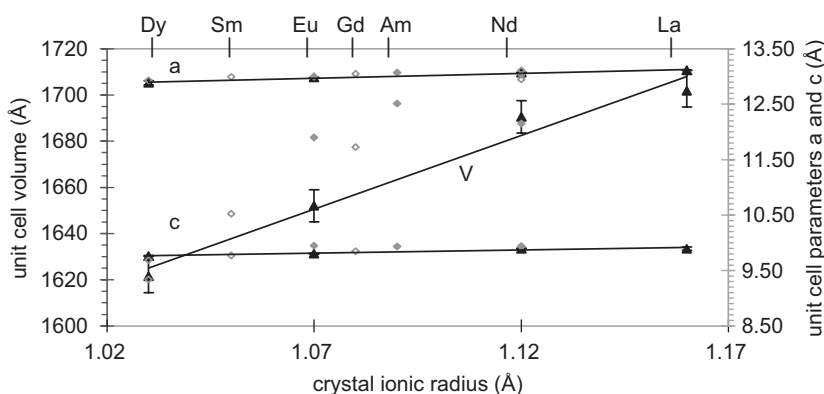


Fig. 6. Relationships between the ionic radii of the lanthanides [45] and the unit cell parameters of the corresponding $\text{NaLn}(\text{CO}_3)_2 \cdot x\text{H}_2\text{O}$ compounds. Our experimental data (solid black triangles) are compared with those of Mochizuki et al. (open grey lozenges) [31] and Runde et al. (solid grey lozenges) [37]. The determined relationships are: $a = (11.10 + 1.75r_{\text{Ln}^{3+}})$, $c = (8.60 + 1.13r_{\text{Ln}^{3+}})$ and $V = (968 + 638r_{\text{Ln}^{3+}})$.

patterns are more different for sodium, lithium and potassium double carbonates. This suggests that the nature of the monocation can be important. Caesium is the biggest cation, and consequently the least reactive towards anions, and the least hydrated in liquid water. This suggests that there is no (or less) bound water in the caesium compounds. The $\text{NH}_4\text{Ln}(\text{CO}_3)_2 \cdot x\text{H}_2\text{O}$ compounds have their own behaviour which seems close to that of $\text{CsLn}(\text{CO}_3)_2 \cdot x\text{H}_2\text{O}$ compounds. Those two mono-cations often have similar behaviours [2].

Runde et al. assigned the most intense peak, i.e. $(h, k, l) = (1, 0, 0)$, to the presence of the intercalated cations and the increased distance between $\text{Ln}(\text{III})$ carbonate layers [37]. $\text{LiEu}(\text{CO}_3)_2 \cdot 3\text{H}_2\text{O}$ and $\text{NaEu}(\text{CO}_3)_2 \cdot 3\text{H}_2\text{O}$ are hydrated by three molecules of bound water whereas $\text{NH}_4\text{Eu}(\text{CO}_3)_2 \cdot \text{H}_2\text{O}$ is hydrated by a single molecule at most. Moreover, the a lattice parameter is shorter for $\text{NH}_4\text{Eu}(\text{CO}_3)_2 \cdot \text{H}_2\text{O}$ than for $\text{LiEu}(\text{CO}_3)_2 \cdot 3\text{H}_2\text{O}$ and $\text{NaEu}(\text{CO}_3)_2 \cdot 3\text{H}_2\text{O}$. This is consistent with our hypothesis concerning the presence of the water in the interlayers. However, the TG analysis did not enable to make the difference between bound and free water for $\text{NH}_4\text{Ln}(\text{CO}_3)_2 \cdot x\text{H}_2\text{O}$ compounds.

Faucherre et al. [33] studied the solubility of $\text{KLn}(\text{CO}_3)_2 \cdot x\text{H}_2\text{O}$ ($\text{Ln} = \text{La}, \text{Pr}, \text{Nd}, \text{Eu}$ and Gd) in $\text{K}_2\text{CO}_3\text{--KHCO}_3\text{--KCl}$ solutions. They reported that the equilibration period between the solid compounds and their mother liquor was less than 3 days. The equilibration period for the solubility measurements were only 24 h, which is certainly not enough to achieve equilibrium. Nevertheless, their results can be qualitatively compared since all the measurements were made using the same procedure. They clearly showed that the solubilities of the double carbonates decrease with the molecular weight of the Ln . This means that the relative stability of the double carbonate compounds increases as compared to that of the aqueous complexes.

The structures of some $\text{ALn}(\text{CO}_3)_2$ single crystals [39,44,49,51] are very different from those of the $\text{ALn}(\text{CO}_3)_2$ polycrystalline powders precipitated at room temperature. Indeed, the single crystals were obtained after heat treatments, and were not equilibrated with aqueous solutions: for this reason, the synthesis of such compounds is out of the scope of the present study. However, these structures give interesting information for the coordination of the Ln^{3+} central atom. In such structures the Ln^{3+} ions are usually octacoordinated or a nanocoordinated to monodentate or bidentate carbonate ligands, and in a few cases to water ligands. The biggest (lightest) lanthanides are expected to be a nanocoordinated. Since the planar triangle carbonate ion is a bridging ligand, the structure of the Ln^{3+} central ion depends on its first and second coordination spheres, the latter is very different in aqueous solutions and in solid compounds. The

structures of $\text{KLn}(\text{CO}_3)_2$ compounds have been published for Nd, Gd, Dy, Ho and Yb [44], to our best knowledge it is the only published work on the structure of $\text{ALn}(\text{CO}_3)_2$ compounds with several lanthanides. In these $\text{KLn}(\text{CO}_3)_2$ compounds the Nd atom is bound to nine O atoms from three bidentate and three monodentate carbonate ligands, whereas Ln is bound to eight O atoms from two bidentate and four monodentate carbonate ligands for $\text{Ln} = \text{Gd}, \text{Dy}, \text{Ho}$ and Yb . The mean distance between the Nd a nanocoordinated central ion and the oxygen atoms is about 2.51 Å whereas it is about 2.37 Å for the heavier octacoordinated Dy central ion. In the latter compound, the $\text{Ln}\text{--O}$ distances are shorter reflecting a higher binding force. The Ln contraction cannot solely explain such a difference in the $\text{Ln}\text{--O}$ distances since $r_{\text{Nd}^{3+}} - r_{\text{Dy}^{3+}} = 0.09 \text{ \AA}$, which is small. However, this illustrates that ionic radii are the key parameter to understand the Ln^{3+} coordination chemistry. The small continuous decrease of the ionic radii within the Ln series is sufficient to stabilise the structures with smaller coordination numbers for the heaviest Ln . It usually explains non-smooth variations of some structural and thermodynamic properties within the Ln series associated with the small Ln contraction, especially the change of the coordination numbers (from 9 to 8) of the aqueous Ln^{3+} cations, and the changes it induces in other physical and chemical properties [54–57]. Our results and published structures suggest that the Ln contraction is also associated with changes in Ln^{3+} coordination geometries and variation of the number of carbonate ligands bound to the central cation, and this changes might explain differences in the kinetic pathways of precipitation.

Acknowledgments

We are grateful to M. Tabarant (ICP-OES) and A. Chénierre (XRD) from CEA/DEN/DANS/DPC/SCP/LRSI; C. Desgranges and S. Bosonet (TG-DTA) from CEA/DEN/DANS/DPC/SCCME/LECNA, F. Onimus (DRX) from CEA/DEN/DANS/DMN/SRMA/LA2M for their technical help and their fruitful experimental advices.

References

- [1] B. Allard, S.A. Banwart, J. Bruno, J.H. Ephram, R. Grauer, I. Grenthe, J. Hadermann, W. Hummel, A. Jakob, T. Karapiperis, A.V. Plyasunov, I. Puigdomenech, J.A. Rard, S. Saxena, K. Spahiu, Modeling in Aquatic Chemistry, Elsevier BV, Amsterdam, 1997.
- [2] P. Vitorge, V. Phrommavanh, B. Siboulet, D. You, T. Vercouter, M. Descostes, C.J. Marsden, C. Beaucaire, J.-P. Gaudet, C. R. Chim. 10 (10–11) (2007) 978–993.
- [3] V. Philippini, Mise en évidence d'un changement de stœchiométrie du complexe carbonate limite au sein de la série des lanthanides(III), Ph.D. Thesis, Paris Sud XI University, France, 2007.

- [4] V. Philippini, T. Vercouter, J. Aupiais, S. Topin, C. Ambard, A. Chausse, P. Vitorge, *Electroporesis 2008*, in press, doi:10.1002/elps.200700764.
- [5] D. Ferri, I. Grenthe, S. Hietanen, F. Salvatore, *Acta Chem. Scand. A* 37 (1983) 359–365.
- [6] P. Robouch, Contribution à la prévision du comportement de l'américium, du plutonium et du neptunium dans la géosphère; données chimiques (thèse), Ph.D. Thesis, Louis Pasteur University, Strasbourg, France, 1987.
- [7] E. Giffaut, Influence des ions chlorure sur la chimie des actinides. Effets de la radiolyse et de la température (thèse), Ph.D. Thesis, Paris Sud XI University, France, 1994.
- [8] L. Rao, D. Rai, A.R. Felmy, R.W. Fulton, C.F. Novak, *Radiochim. Acta* 75 (1996) 141–147.
- [9] T. Vercouter, P. Vitorge, N. Trigoulet, E. Giffaut, C. Moulin, *N. J. Chem.* 29 (2005) 544–553.
- [10] P. Vitorge, *Radiochim. Acta* 58–59 (1992) 105–107.
- [11] I.N. Tselik, G.F. Deineka, V.D. Fedorenko, V.Y. Schvartsman, *Russ. J. Inorg. Chem.* 14 (9) (1969).
- [12] G.F. Deineka, I.N. Tselik, E.P. Il'inskaya, *Russ. J. Inorg. Chem.* 17 (5) (1972) 670–672.
- [13] N.V. Mzareulishvili, *Soobshch. Akad. Nauk Gruz. SSR* 67 (3) (1972) 593–596 (in Russian).
- [14] N.V. Mzareulishvili, E.G. Davitashvili, V.P. Natidze, *Soobshch. Akad. Nauk Gruz. SSR* 75 (3) (1974) 601–604 (in Russian).
- [15] N.V. Mzareulishvili, E.G. Davitashvili, V.P. Natidze, *Obl. Khim. Kompleksn. Prostykh. Soedin. Nek. Perekhodnykh Redk. Met.*, vol. 2, 1974, pp. 226–230 (in Russian).
- [16] N.V. Mzareulishvili, V.P. Natidze, *Izv. Akad. Nauk Gruz. SSR Ser. Khim.* 2 (1) (1976) 14–21 (in Russian).
- [17] L.V. Ruzaikina, I.N. Marov, V.A. Ryabukhin, A.N. Ermakov, V.N. Filimova, *Zh. Anal. Khim.* 33 (6) (1978) 1082–1088 (in Russian).
- [18] N.V. Mzareulishvili, V.P. Natidze, *Soobshch. Akad. Nauk Gruz. SSR* 126 (1) (1987) 81–84 (in Russian).
- [19] K. Nagashima, H. Wakita, A. Mochizuki, *Bull. Chem. Soc. Jpn.* 46 (1973) 152–156.
- [20] F. Fromage, *Ann. Chim.* 3 (1968) 457–467 (in French).
- [21] I.N. Tselik, G.F. Deineka, V.D. Fedorenko, V.Y. Schvartsman, *Ukr. Khim. Zh.* 35 (35) (1969) 1042–1045 (in Russian).
- [22] I.N. Tselik, G.F. Deineka, V.D. Fedorenko, *Russ. J. Inorg. Chem.* 15 (8) (1970) 1166–1168.
- [23] N.V. Mzareulishvili, E.G. Davitashvili, V.P. Natidze, *Soobshch. Akad. Nauk Gruz. SSR* 62 (3) (1971) 573–576 (in Russian).
- [24] N.V. Mzareulishvili, E.G. Davitashvili, *Soobshch. Akad. Nauk Gruz. SSR* 49 (2) (1968) 351–356 (in Russian).
- [25] V.A. Golovnya, L.A. Pospelova, *J. Inorg. Chem. USSR* (1958) 37–46.
- [26] N.V. Mzareulishvili, V.P. Natidze, *Soobshch. Akad. Nauk Gruz. SSR* 121 (1) (1986) 81–84 (in Russian).
- [27] N.V. Mzareulishvili, E.G. Davitashvili, V.P. Natidze, *Izv. Akad. Nauk Gruz. SSR Ser. Khim.* 9 (3) (1983) 172–175 (in Russian).
- [28] N.V. Mzareulishvili, V.P. Natidze, H.N. Zedelashvili, *Izv. Akad. Nauk Gruz. SSR Ser. Khim.* 72 (2) (1973) 345–348 (in Russian).
- [29] N.V. Mzareulishvili, *Soobshch. Akad. Nauk Gruz. SSR* 137 (2) (1990) 309–312 (in Russian).
- [30] N.V. Mzareulishvili, E.G. Davitashvili, V.P. Natidze, *Izv. Akad. Nauk Gruz. SSR Ser. Khim.* 9 (2) (1983) 91–96 (in Russian).
- [31] A. Mochizuki, K. Nagashima, H. Wakita, *Bull. Chem. Soc. Jpn.* 47 (3) (1974) 755–756.
- [32] C.A. Fannin, The rare earth elements as natural analogues for the actinides, Ph.D. Thesis, Liverpool John More University, UK, 1999.
- [33] J. Faucherre, F. Fromage, R. Gobron, *Rev. Chim. Minér* 3 (1966) 953–991 (in French).
- [34] H.-J. Von Kalz, H. Seidel, *Z. Anorg. Allg. Chem.* 465 (1980) 92–108 (in German).
- [35] V.H. Schweer, H. Seidel, *Z. Anorg. Allg. Chem.* 477 (1981) 196–204 (in German).
- [36] H.-J. Kalz, H. Seidel, *Z. Anorg. Allg. Chem.* 486 (1982) 221–228 (in German).
- [37] W. Runde, C. Van Pelt, P.G. Allen, *J. Alloys Comp.* 303–304 (2000) 182–190.
- [38] M. Irmiler, C. Koepfeland, H. Bergmann, *Gmelin Handbook of Inorganic and Organometallic Chemistry, Rare Earth Elements, C 12b, Compounds with Carbon*, Springer, New York, 1994.
- [39] W. Runde, M.P. Neu, C. Van Pelt, B.L. Scott, *Inorg. Chem.* 39 (2000) 1050–1051.
- [40] C. Fannin, R. Edwards, J. Pearce, E. Kelly, *Appl. Geochem.* 17 (2002) 1305–1312.
- [41] R.G. Charles, *J. Inorg. Nucl. Chem.* 27 (1965) 1489–1493.
- [42] M.S. Wickleder, *Chem. Rev.* 102 (6) (2002) 2011–2087.
- [43] J. Delaunay, A. de Polignac, F. Fromage, J. Despujols, *C. R. Acad. Sci.* 273 (1971) 692–695 (in French).
- [44] I. Kutlu, H.-J. Kalz, R. Wartchow, H. Ehrhardt, H. Seidel, G. Meyer, *Z. Anorg. Allg. Chem.* 623 (1997) 1753–1758 (in German).
- [45] R.C. Weast, *CRC Handbook of Chemistry and Physics, 83rd ed.*, CRC Press, Boca Raton, FL, 2002.
- [46] F. David, *J. Less-Common Met.* 121 (1986) 27–42.
- [47] E.N. Rizkalla, G.R. Choppin, Lanthanides and actinides hydration and hydrolysis, in: *Handbook on the Physics and Chemistry of Rare Earths*, vol. 18: Lanthanides/Actinides Chemistry, North Holland, Amsterdam (Chapter 127).
- [48] V. Philippini, T. Vercouter, A. Chausse, P. Vitorge, Evidence of different stoichiometries for the limiting carbonate complexes across the lanthanide(iii) series: a solubility study, in preparation.
- [49] A. Lossin, G. Meyer, *Z. Anorg. Allg. Chem.* 619 (1993) 2031–2037 (in German).
- [50] M. Evain, U-Fit: A Cell Parameter Refinement Program, Institut de Matériaux de Nantes, France, 1992.
- [51] I. Kutlu, G. Meyer, *Z. Kristallogr. N. Cryst. Struct.* 213 (2) (1998) 236.
- [52] A.A. Voronkov, Y.A. Pyatenko, *Zh. Strukt. Khim.* 8 (5) (1967) 935–942 (in Russian).
- [53] S. Liu, R.J. Ma, *J. Cryst. Growth* 169 (1) (1996) 190–192.
- [54] G.R. Choppin, A.J. Graffeo, *Inorg. Chem.* 4 (9) (1965) 1254–1257.
- [55] S.L. Bertha, G.R. Choppin, *Inorg. Chem.* 8 (3) (1969) 613–617.
- [56] A. Habenschuss, F.H. Spedding, *J. Chem. Phys.* 70 (8) (1979) 3758–3763.
- [57] A. Habenschuss, F.H. Spedding, *J. Chem. Phys.* 70 (6) (1979) 2797–2806.